International Journal of Thermophysics, Vol. 20, No. 4, 1999

Graphite Melting and Properties of Liquid Carbon[1]

V. N. Korobenko,[2] A. I. Savvatimski,[2, 3] and R. Cheret[4]

The results of fast heating (by electrical pulse current) of highly oriented pyrolytic graphite specimens are presented. Experimental data are obtained for graphite melting: the enthalpy of solid and liquid phases under melting, the heat of melting, and the heat capacity of solid and liquid phases near melting. Liquid carbon resistivity is measured under fast heating of cylindrical graphite specimens in thick-walled sapphire capillary tubes. Preliminary data for the isobaric heat capacity C_p for liquid carbon up to 10,000 K and for the isochoric heat capacity C_v up to 8000 K are presented.

KEY WORDS: carbon; fast heating; graphite; heat capacity; high temperature; liquid carbon; melting; pulse current; pyrometer; thermophysical properties.

1. INTRODUCTION

There are several experimental data in the literature for the thermophysical properties of graphite under melting [1–6]. Some problems for the properties of graphite under melting have not yet been resolved; these include high-quality measurements of the complete temperature plateau during melting and the value of the liquid carbon resistivity.

In this paper a method for investigating the properties of liquid carbon is presented. The capillary method is used, which was earlier applied to liquid metal investigations [7, 8]. The method of restricted volume around the specimen is also used. It is used to avoid sublimation of graphite under high temperatures (5000–10,000 K) and under fast heating (near 1 μs).

---

[1] Paper presented at the Fifth International Workshop on Subsecond Thermophysics, June 16–19, 1998, Aix-en-Provence, France.

[2] Department of Experimental Thermophysics, High Energy Density Research Center, United Institute of High Temperature, Russian Academy of Sciences, Izhorskaya 13/19, 127412 Moscow I-412, Russia.

[3] To whom correspondence should be addressed.

[4] Commissariat à l'Energie Atomique (CEA), BP 12, 91680 Bruyères-le-Chatel, Paris, France.

2. EXPERIMENTAL

2.1. Specimens

The specimens of highly oriented graphite structure had the parameters **a** $= 0.2462$ nm and **c** $= 0.6706$ nm. The average crystallite size in both directions was near 2000 nm. These values were measured by the X-ray diffraction method. The X-ray density was $2.265\ \mathrm{g \cdot cm^{-3}}$, and the volume density was $2.25\ \mathrm{g \cdot cm^{-3}}$. The specimen had cross-sectional dimensions of 0.66×0.38 mm and a length of 11.2 mm. The specimen in the form of a strip was placed in transparent Canadian balsam, between two glasses (each 3 mm thick). The initial graphite resistivity was near $50\ \mu\Omega \cdot \mathrm{cm}$.

In Fig. 1 are plotted the voltage U across the strip graphite specimen (in arbitrary units), the temperature T (the change of spectral emissivity is

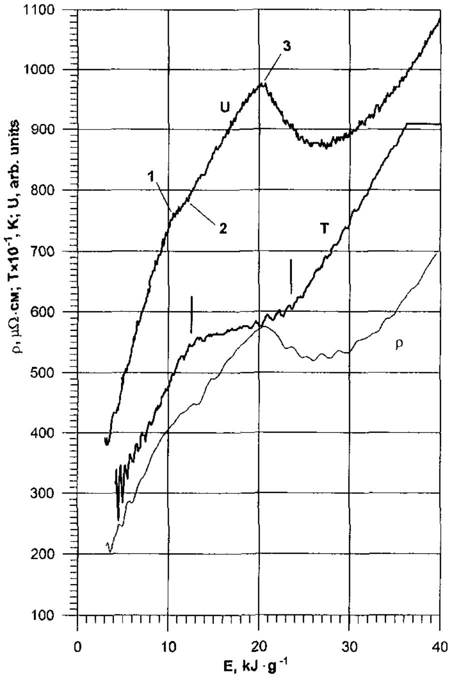

Fig. 1. Dependence of voltage across the specimen (U), temperature (T), and resistivity (ρ) on imparted energy (E) under pulse electrical heating of the graphite strip. The two vertical lines mark the melting region. The resistivity ρ is referenced to the initial dimensions of the specimen.

not included), and the resistivity ρ, referenced to the initial length and cross section of the specimen as functions of the imparted energy (E) under pulse electrical heating of the graphite strip. The imparted energy (E) was measured using the oscilloscope data of the voltage, current, time, and specific weight of the specimen. According to evaluations, the imparted energy (E) is the same as the enthalpy in our fast experiment.

2.2. Results

A specimen was placed in hard cover as noted above. Fast pyrometry was used based on a PIN photodiode with a transimpedance amplifier. It was focused on plane **a** (width, 0.66 mm) by means of a lens. The diameter of the visible spot on the specimen's side was approximately 0.5 mm. A digital oscilloscope (Tektronix TDS640A) with four channels was used for measurement of the voltage across the specimen, the current through it, and the surface temperature. Determination of the temperature was based on measuring the radiance from the graphite surface (**a**-plane) at a wavelength of 900 ± 8 nm. Temperatures were calculated using Plank's equation. Calibration of the pyrometer signal was made at an imparted energy of $9.14\ \mathrm{kJ \cdot g^{-1}}$ (relatively to room temperature), where the temperature of graphite $T = 4500$ K according to Ref. 9. Figure 1 shows the temperature dependence of the enthalpy (unfitted curve). This curve had an oblique plateau in the range of enthalpies from 12.5 to $23.5\ \mathrm{kJ \cdot g^{-1}}$ (two vertical lines mark the plateau region). The heat of melting is $11\ \mathrm{kJ \cdot g^{-1}}$. One can see in Fig. 1 that the melting graphite temperature is equal to 5500 K.

The isobaric heat capacity C_p of solid graphite before melting (Fig. 1) is equal to $3.2\ \mathrm{J \cdot g^{-1} \cdot K^{-1}}$ (for T from 4200 to 5200 K). Literature results [10] give a value of $3.27\ \mathrm{J \cdot g^{-1} \cdot K^{-1}}$ at $T = 4400$ K, which increases to $4.11\ \mathrm{J \cdot g^{-1} \cdot K^{-1}}$ for $T = 4900$ K (melting temperature). In Ref. 9 the values are $3.08\ \mathrm{J \cdot g^{-1} \cdot K^{-1}}$ for $T = 4200$ K and $3.77\ \mathrm{J \cdot g^{-1} \cdot K^{-1}}$ for $T = 4500$ K. Under pulse heating, Ref. 3 gives a value of $3.12\ \mathrm{J \cdot g^{-1} \cdot K^{-1}}$ for $T = 4500$ K. Thus, our result for the isobaric heat capacity C_p of solid graphite before melting ($3.2\ \mathrm{J \cdot g^{-1} \cdot K^{-1}}$) is quite close to literature values.

The heat capacity of liquid carbon in this experiment (Fig. 1) is equal to $4\ \mathrm{J \cdot g^{-1} \cdot K^{-1}}$ for T from 7000 to 8500 K. Other curves in Fig. 1 show the smoothed dependence of resistivity ρ and unfitted dependence of voltage U on the enthalpy E.

The average of six experiments with six specimens (strip form) gives the final result. The enthalpy of the solid state under melting $H_s = 12 \pm 1\ \mathrm{kJ \cdot g^{-1}}$. The enthalpy of the liquid state under melting $H_l = 23 \pm 1\ \mathrm{kJ \cdot g^{-1}}$. The heat of melting $\Delta H = 11 \pm 1\ \mathrm{kJ \cdot g^{-1}}$. The resistivity of solid graphite at the melting point $\rho_s = 420 \pm 40\ \mu\Omega \cdot \mathrm{cm}$. The resistivity of the liquid phase at the melting point $\rho_l = 560 \pm 40\ \mu\Omega \cdot \mathrm{cm}$.

There are two unusual points that occur before melting, marked 1 and 2 on the voltage curve since it has a small scatter (Fig. 1). Point 1 occurs somewhat ahead of the beginning of melting. Point 2 practically coincides with the onset of melting determined by the temperature plateau. Point 3 (on the dependence of U on the enthalpy) shows the moment at which the sign of the derivative of electrical resistivity changes. This change has two possible explanations. It may result from a decrease in resistivity ρ itself, or it may result from an expansion of the cross section of the specimen. This expansion would lead to a decrease in the resistivity, with no volume correction. Additional experiments showed that the second supposition was true.

These experiments needed new specimens. In the control experiments, thick-walled sapphire capillary tubes were used, which have an outer diameter of 12 mm. A special method was used to prepare new specimens (length, 15 mm) from the same block of high quality graphite in a circular form. The diameter of these new specimens was 0.87 mm. The hole in the thick-walled sapphire capillary tubes was 0.97 mm in diameter. Thus, the ratio of the cross sections (volumes) of the tubes V_c and the specimen V_0 was $V_c / V_0 = 1.24$.

The results for the circular cross-section specimens (Curve 2), restricted by the free-volume tube, are presented in Fig. 2. Curve 1 designates the dependence of ρ for the strip specimen (the same as in Fig. 1). Vertical lines show the start and finish of melting for specimen 1 from Fig. 1. One can imagine that the decrease in resistivity ρ for specimen 1 (no volume correction) from 570 to $520\ \mu\Omega \cdot \mathrm{cm}$ (Fig. 2) corresponds to the increase of 4.5% in the cross-sectional area of the strip specimen. The expansion of the specimen along its length is negligible and is not included in the calculations.

One can also see in Fig. 2 that the resistivity of liquid carbon (taking into account the thermal expansion of the circular specimen up to the internal capillary volume) is represented by Curve 2: $\rho_l = 590\ \mu\Omega \cdot \mathrm{cm} \times 1.24 = 730\ \mu\Omega \cdot \mathrm{cm}$. The corresponding value for the solid state at the melting point is $\rho_s = 465\ \mu\Omega \cdot \mathrm{cm} \times 1.20 = 558\ \mu\Omega \cdot \mathrm{cm}$ (taking into account literature data on the thermal expansion of graphite). The ratio of change of resistivity on melting is $\rho_l / \rho_s = 1.3$. These results do not take into account the possible expansion of the sapphire tube in the solid elastic region. The further increase in ρ after melting is probably due to the destruction of the sapphire tube and, hence, expansion of the specimen.

Figure 3 shows three fitted curves of the temperature T dependence upon the imparted energy E for three pulse experiments. All three specimens were of the strip form, packed between two glasses as discussed

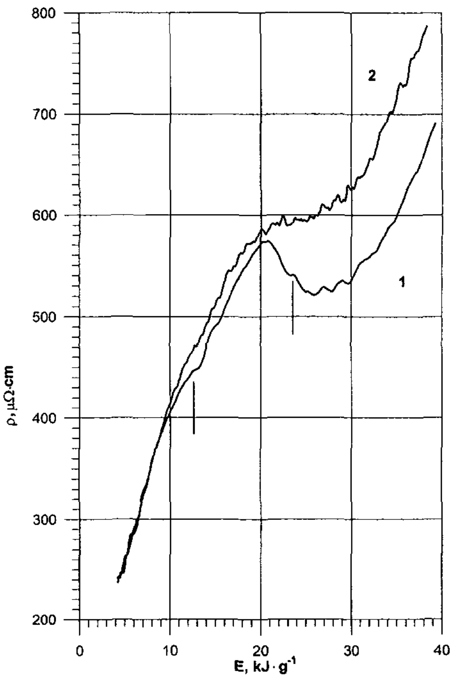

Fig. 2. Resistivity ρ (referenced to the initial dimensions of a specimen) versus the imparted energy E. (1) Specimen in strip form. The two vertical lines mark the melting region. (2) Specimen in cylindrical form (diameter of 0.87 mm), heated in a thick-walled sapphire capillary tube.

above for Fig. 1. Very large instabilities appeared in Curve 3 (the slowest-heating specimen) in the liquid phase due to the long interaction with the cell wall. The upper levels of 1–3 dependences were limited by the dynamic range of the oscilloscope channel.

Previous results of Butchnev et al. [10] for the solid state of graphite (Curve 4) up to 4900 K are shown in Fig. 3 for quasi-monocrystal graphite UPV-1T. The current results agree with the temperature dependence in Ref. 9 up to 4500 K for the same graphite. The experimental data from this work for the solid state of graphite are in good agreement with literature data [9, 10].

Figure 4 shows the dependence of temperature on the imparted energy for the wide range of the liquid state. The data for two experiments (under the same heating rate) demonstrate the possibilities of liquid carbon investigation. The specimens are in strip form. The difference in temperatures for

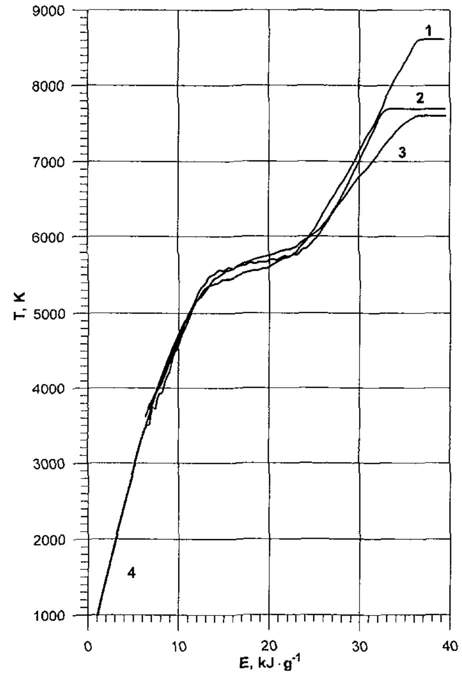

Fig. 3. Dependence of temperature T on imparted energy E for the solid phase of graphite and for the region of melting. (1) Specimen in Fig. 1. (2) Specimen with the following dimensions: thickness $\delta = 0.365$ mm; width $h = 0.65$ mm; length $l = 11.6$ mm; mass $m = 6.03$ mg. (3) $\delta = 0.32$ mm; $h = 0.95$ mm; $l = 11.9$ mm; $m = 8.16$ mg. (4) Steady-state measurement data for quasi-monocrystal graphite UPV-1T for temperatures up to 4900 K [10], which practically coincide with data from Ref. 9 up to 4500 K for the same kind of graphite.

two experiments under an imparted energy of 40 kJ · g^{-1} ($T \cong 10{,}000$ K) is approximately 3%. The estimated error of temperature measurement is much greater, about 10%. The isobaric heat capacity $C_p = 3.7$ kJ · g^{-1} · K^{-1} for temperatures from 8500 to 11,000 K. Figure 4 shows the wide range of the liquid carbon state up to temperatures near 12,000 K.

The dependence of temperature on enthalpy was determined for the cylindrical specimen (made from the same monocrystal block) with a diameter of 0.87 mm. The specimen was placed inside the thick-walled sapphire tube ($d/D = 0.97/11$ mm). The ratio $V_c/V_o = 1.25$. The surface

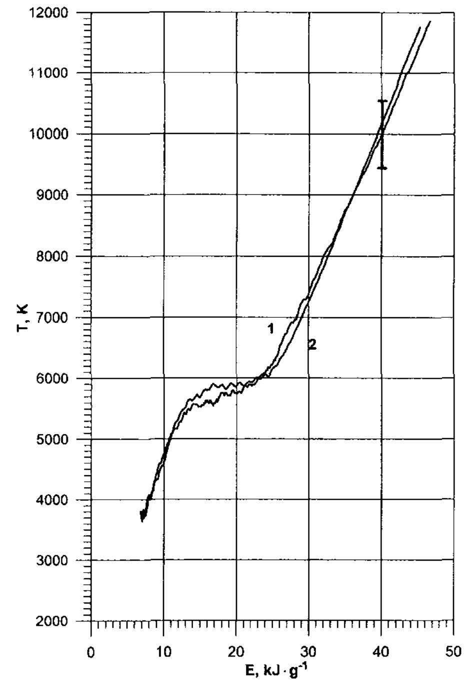

Fig. 4. Dependence of temperature T on imparted energy E for liquid carbon.

temperature of the "black" c-side was measured through the sapphire wall. For this case a piece of flat glass was placed on the outer surface of the sapphire tube using optical glue. The optical pyrometer showed (Fig. 5) that the melting started at 10.5 to 11 $\mathrm{kJ \cdot g^{-1}}$ ($T = 5000$ K) and finished at 21.5 to 22 $\mathrm{kJ \cdot g^{-1}}$. It should be mentioned that these measurements for the start of melting agree with the well-known measurements of Ref. 3. As a result, the heat of melting was 11 $\mathrm{kJ\, g^{-1}}$, as was obtained for strip specimens.

The two vertical lines in Fig. 5 designate the melting region. Figure 5 shows the resistivity ρ as a function of the enthalpy (without volume correction). The value of the liquid carbon resistivity is approximately 590 $\mu\Omega \cdot \mathrm{cm}$, in agreement with the previous experiments with the other cylindrical graphite specimens. As the liquid carbon was in a restricted volume just after melting (assuming the expansion of the sapphire tube to be negligible), the value of the isochoric heat capacity C_v may be determined. The isochoric heat capacity of liquid carbon at several kilobars of

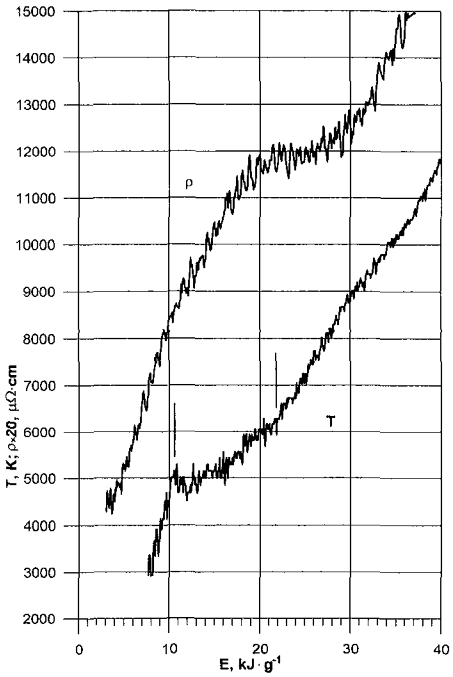

Fig. 5. Melting of quasi-monocrystal cylindrical graphite in a thick-walled sapphire tube. The two vertical lines mark the melting region.

pressure, $C_v = 3\ \mathrm{J \cdot g^{-1} \cdot K^{-1}}$, up to approximately 8000 K. Thus, the ratio C_p/C_v for liquid carbon is approximately 4/3, or 1.3.

Efforts were made to check the influence of the aperture in measuring the temperature dependence of enthalpy during graphite melting. Figure 6 shows the pyrometer signal (but not temperature) of a highly oriented graphite strip placed in a flat sapphire cell. The radiance of a small spot (diameter, 0.25 mm) from surface "**a**" is also shown in Fig. 6. The plateau of melting now has a nearly constant value. The electrical resistivity (with no volume correction) is shown. Unfortunately, the value of the pyrometer signal is rather small to make a temperature calibration level at $9.14\ \mathrm{kJ \cdot g^{-1}}$ ($T = 4500$ K).

3. CONCLUSION

The electrical resistivity of liquid carbon at the melting point (without volume correction) is $590\ \mu\Omega \cdot \mathrm{cm}$, and the electrical resistivity (with

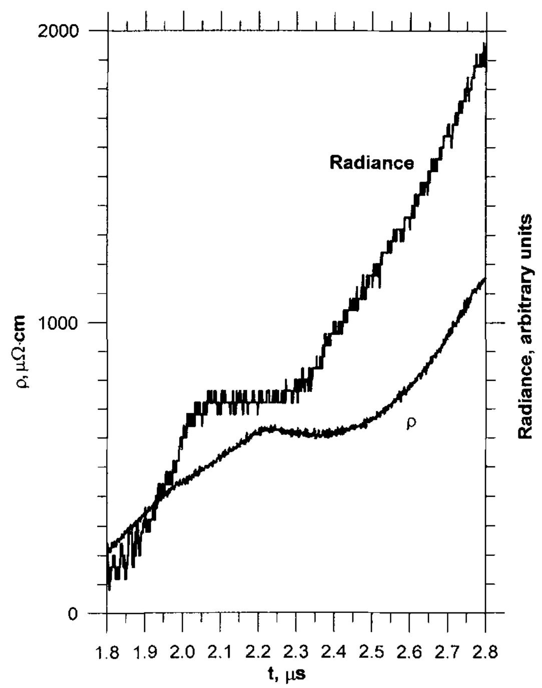

Fig. 6. Pyrometer signal (radiance from a small spot, 0.25-mm diameter, on surface "**a**" of a highly oriented graphite strip, placed in a flat sapphire cell) and resistivity of graphite (no volume correction).

volume correction) is 730 $\mu\Omega \cdot$cm. The enthalpy of solid graphite at the melting point H_s is $11 \div 12$ kJ $\cdot$ g^{-1}. The graphite heat of melting is 11 kJ $\cdot$ g^{-1}.

Preliminary values of the heat capacity of liquid carbon are as follows: $C_p = 3.7$ to 4 J $\cdot$ g^{-1} $\cdot$ K^{-1} and $C_v = 3$ J $\cdot$ g^{-1} $\cdot$ K^{-1}.

ACKNOWLEDGMENTS

This work was supported by the CEA Centre (France), Contract CEA/DAM, No. 3665/DIR, and also by the Russian Fund for Fundamental Investigation (RFFI), Scientific Research Grant 98-02-16278.

REFERENCES

1. F. P. Bundy, *J. Chem. Phys.* **38**:618 (1963).
2. S. V. Lebedev and A. I. Savvatimski, *Teplofiz. Visokih Temp.* **24**:892 (1986).

3. M. A. Sheindlin and V. N. Senchenko, *Doklady Akad. Nauk (Fizika)* **298**:1383 (1988).
4. A. Cezairliyan and A. P. Miiller, *Int. J. Thermophys.* **11**:643 (1990).
5. A. V. Baitin, A. A. Lebedev, S. V. Romanenko, V. N. Senchenko, and M. A. Sheindlin, *High Temp.-High Press.* **21**:157 (1990).
6. G. Pottlacher, R. S. Hixson, S. Melnitzky, E. Kaschnitz, M. A. Winkler, and H. Jager, *Thermochim. Acta* **218**:183 (1993).
7. S. V. Lebedev and A. I. Savvatimski, *Uspekhi Fiz. Nauk.* **144**:215 (1984).
8. A. I. Savvatimski, *Int. J. Thermophys.* **17**:495 (1996).
9. G. A. Bergman, L. M. Butchnev, I. I. Petrova, V. N. Senchenko, L. R. Fokin, V. Ya. Chekhovskoi, and M. A. Sheindlin, in *Tablitsy standartnykh spravochnykh dannykh (State Service of Standard Referee Data)*, Grafit kvazimonokristallicheskii, Moscow, GSSD 25-90 (1991).
10. L. M. Butchnev, A. I. Smyslov, I. A. Dmitriev, A. F. Kuteinikov, and V. I. Kostikov, *Teplofiz. Visokih Temp.* **25**:1120 (1987).